Cell Reports, Volume *42*

Supplemental information

Deep mutational scanning highlights a role for cytosolic regions in Hrd1 function

Brian G. Peterson, Jiwon Hwang, Jennifer E. Russ, Jeremy W. Schroeder, P. Lydia Freddolino, and Ryan D. Baldridge

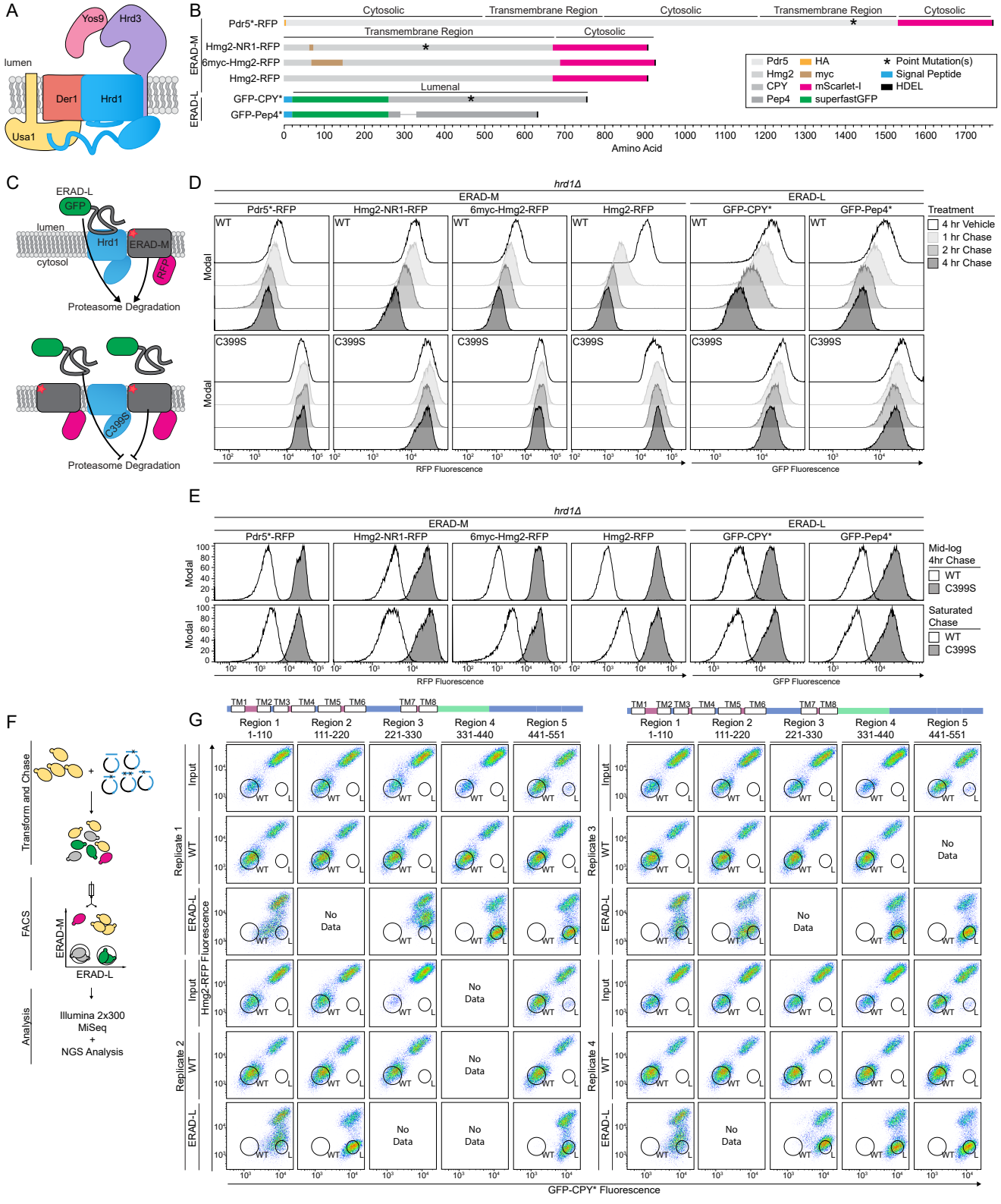

Figure S1. Deep mutation scanning screen development, related to Figure 1

(Legend Next Page)

Figure S1. Deep mutation scanning screen development, related to Figure 1
(A) Hrd1 complex schematic. **(B)** Schematic of fluorescent ERAD substrates. RFP represents mScarlet-I[S1] and GFP represents superfastGFP.[S2] Pdr5* is a mutated ATP-binding cassette transporter with a HA epitope tag inserted between Pro2 and Glu3 that is rendered ERAD-M substrate by a C1427Y mutation.[S3, 4] There are three different versions of Hmg2 that behave as ERAD-M substrates. Hmg2 represents wild-type Hmg2's transmembrane region (Met1 to Tyr670) where degradation is regulated by the mevalonate pathway.[S5] Hmg2-NR1 contains a myc tag replacing Thr61 through Leu70, and is rendered unresponsive to metabolites in the mevalonate pathway by replacing Thr348 through Ala352 in the sterol sensing domain with a five amino acid substitution (Ile-Leu-Gln-Ala-Ser); this substitution causes Hmg2-NR1 to be constitutively turned over.[S6] Finally, 6myc-Hmg2 is a grossly misfolded Hmg2 generated by replacing Ser64 through Glu145 with six tandem myc tags.[S5] For ERAD-L substrates, we used CPY* and Pep4*. CPY* is a lumenal vacuolar protease that is rendered a ERAD-L substrate by a single missense mutation of G255R.[S7] Pep4* is also a lumenal vacuolar protease that is rendered an ERAD-L substrate by deletion of 37 amino acids from Leu55 through Tyr91.[S7] **(C)** Model for fluorescent ERAD reporter proteins. Top: Wild-type Hrd1 degrades fluorescent reporters at the proteasome. Bottom: A RING-finger mutation inactivates Hrd1 (Hrd1(C399S)) causes substrates to accumulate. **(D)** Degradation of the indicated ERAD substrates were followed using flow cytometry after the addition of 0.1% ethanol (vehicle control), 10 µg/mL zaragozic acid (for Hmg2), or 50 µg/mL cycloheximide (for CPY*). Experiments were performed in *hrd1*Δ cells complemented with either wild-type Hrd1(WT) or a RING domain mutant Hrd1(C399S). Histograms are scaled as a percentage of maximum cell count (Modal). **(E)** Substrate degradation was followed using flow cytometry during either mid-log phase growth treated as in (D) (Mid-log Chase, top panels) or with cells grown to saturation and no pharmacological treatment (Saturated Chase, bottom panels). **(F)** Schematic of deep mutational scanning screen. Yeast cells expressing integrated substrates were transformed with a PCR product containing tiling primer mutagenized region of Hrd1 and linearized centromeric plasmid backbone. Transformed cells were grown in liquid culture and subjected to a saturated chase. Wildtype-like cells and ERAD-L defective cells were sorted using FACS. Sorted cells had their phenotype validated before DNA extraction, library preparation, Illumina sequencing, and analysis. During screening optimization, yeast cells expressed substrates from centromeric plasmids and individual colonies were isolated, phenotype validated, and Sanger-sequenced. **(G)** Phenotype confirmation for previously isolated FACS populations following outgrowth (from figure 1D). Top: topology diagram of Hrd1 with transmembrane segments shown as TM1-8. Cytosolic and lumenal segments are shown as blue and magenta respectively. The cytosolic RING domain is shown in green. Bottom: Input library (Input), the wildtype-like sorted population (WT) or ERAD-L defective sorted population were subjected to a saturated chase. The results are displayed as pseudo color flow cytometry plots of GFP-CPY* (x-axis) and Hmg2-RFP (y-axis). Replicate 1 and 2 are on the left set of panels; Replicate 3 and 4 are on the right set of panels. Missing replicates highlighted as "No Data".

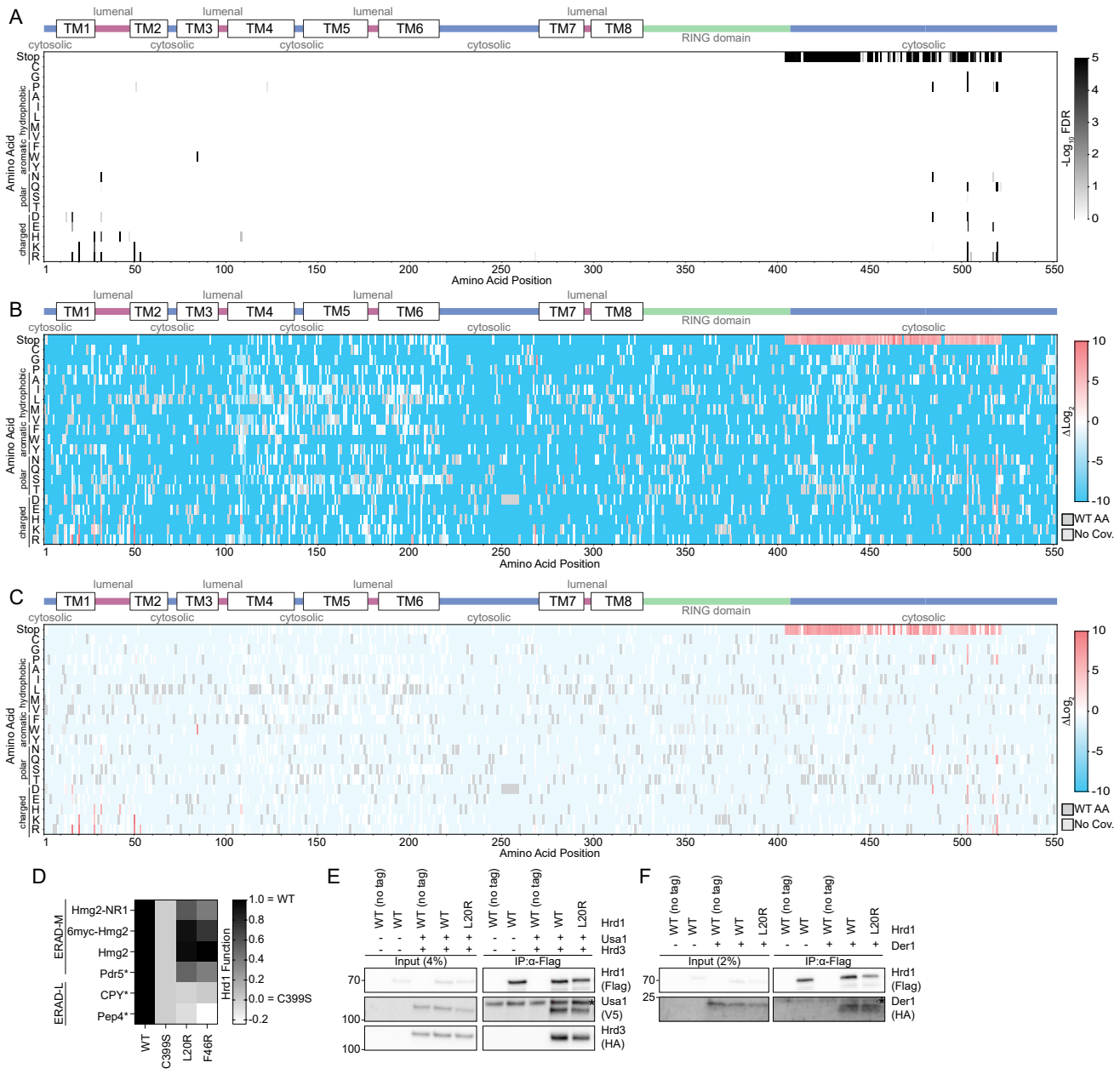

Figure S2. ERAD-L defective DMS results, related to Figure 2

(A) Top: Topology diagram of Hrd1 with transmembrane segments shown as TM1-8. Colors indicate the cytosolic (blue), lumenal (magenta), and cytosolic RING domain (green). Bottom: Deep mutational scanning results of cells sorted into the ERAD-L defective bins displayed as a heatmap showing -log$_{10}$(false discovery rate (FDR)). Wild-type amino acids and lack of coverage were omitted for clarity. Related to (Figure 2A). **(B)** As in (A) but showing ERAD-L defective enrichment values. FDR is not used to adjust transparency. (Next Page)

Figure S2. ERAD-L defective DMS results, related to Figure 2

(C) As in (A) but showing ERAD-L defective enrichment values. Transparency was adjusted based on FDR. FDR below 0.1% were set to 0% transparent and FDR values between 0.1% to 100% were used to adjust transparency from 0% (opaque) to 90% transparent. Individual amino acids are on the y-axis, and the Hrd1 amino acid position is on the x-axis. Dark gray boxes indicate the wild-type amino acid and light gray boxes indicate lack of coverage. **(D)** Degradation of ERAD substrates by individual Hrd1 variants were followed by flow cytometry and summarized in a heatmap. The indicated Hrd1 variants were integrated in *hrd1Δ* cells expressing individual ERAD substrates and subjected to a 4-hour mid-log chase. Wild-type Hrd1(WT) is set to 1 (full function) and inactive Hrd1(C399S) is set to 0 (no function). Related to (Figure 2F). **(E)** Co-immunoprecipitation of the Hrd1 complex was performed with the indicated Hrd1 variants. 3xHA-Hrd3, 3xV5-Usa1, and Hrd1-3xFlag were integrated into *hrd1Δhrd3Δusa1Δ* cells, lysed, and immunoprecipitated with anti-Flag antibodies. Input represents 4% of the cleared lysate. These immunoblots are representative of 3 independent replicates. "*" indicates a nonspecific band. **(F)** Co-immunoprecipitation of the Hrd1 complex was performed with the indicated Hrd1 variants. Hrd1-3xFlag was integrated into *hrd1Δder1Δ* cells, and Der1-HA was expressed from a centromeric plasmid. Cells were lysed and immunoprecipitated with anti-Flag antibodies. Input represents 2% of the cleared lysate. These immunoblots are representative of 3 independent replicates. "*" indicates a nonspecific band.

For this figure, the number of quantified replicates and individual values are shown in Table S8.

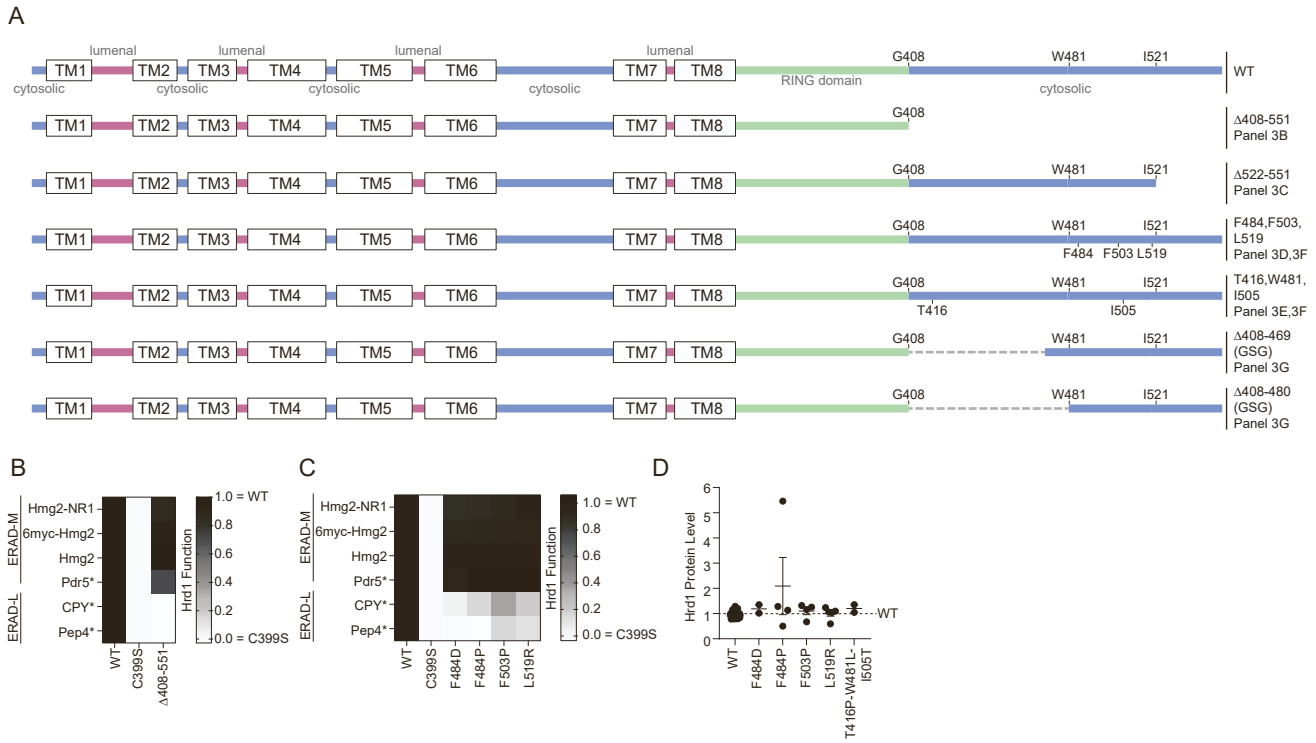

Figure S3. Degradation and protein stability profiles of Hrd1 C-terminal mutants, related to Figure 3

(A) Topology diagram of Hrd1(WT) and Hrd1 variants used in Figure 3. Transmembrane segments are displayed as TM1-8. Colors indicate the cytosolic (blue), lumenal (magenta), and cytosolic RING domain (green). Regions replaced by a Gly-Ser-Gly (GSG) linker indicated by gray dashes. **(B)** Degradation of ERAD substrates by individual Hrd1 variants were followed by flow cytometry and summarized in a heatmap. The indicated Hrd1 variants were integrated in *hrd1Δ* cells expressing individual ERAD substrates and subjected to a 4-hour mid-log chase. Wild-type Hrd1(WT) is set to 1 (full function) and inactive Hrd1(C399S) is set to 0 (no function). Related to (Figure 3B). **(C)** As in (B), related to (Figure 3D) **(D)** Expression levels of Hrd1 variants were determined by immunoblotting. *hrd1Δ* cells expressing indicated Hrd1-3xFlag constructs were normalized to wild-type Hrd1(WT) (1-black dash line). Total protein was visualized by stain-free technology as a loading control. Results are displayed as the mean +/- SEM. Individual values are biological replicates.

For this figure, the number of quantified replicates and individual values are shown in Table S8 and S9.

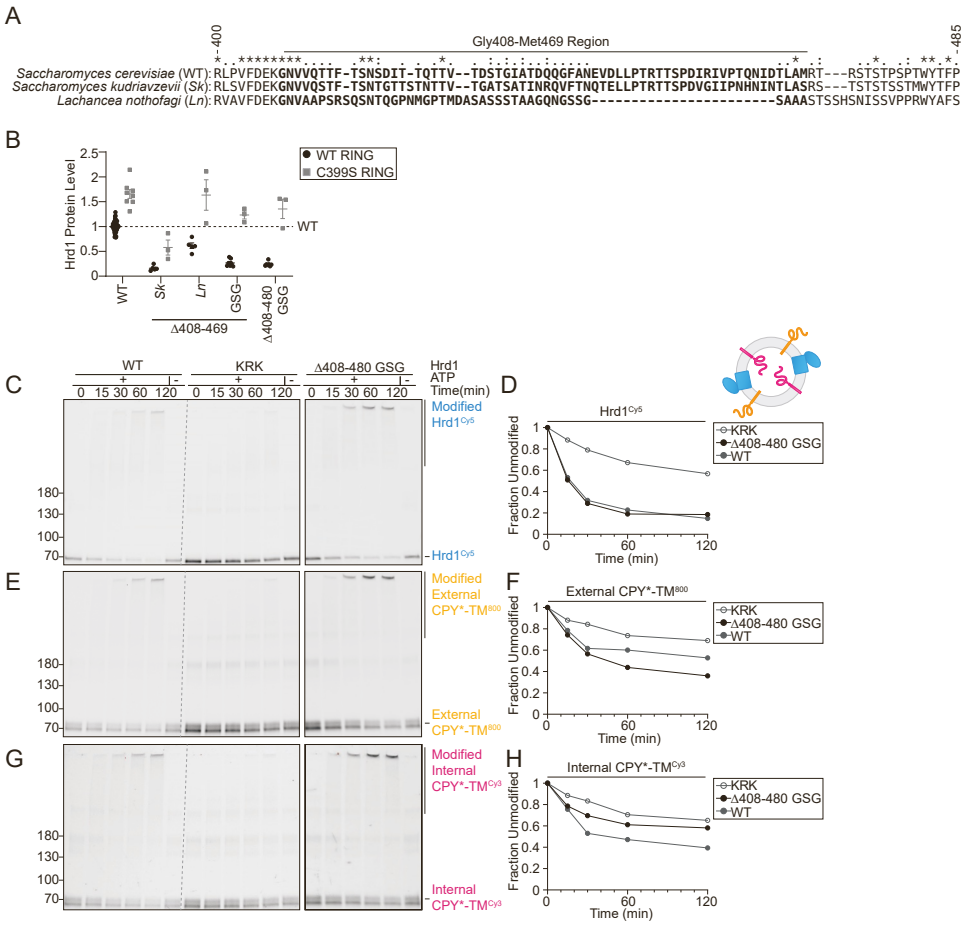

Figure S4. Alignment of divergent Hrd1s and Hrd1(*Δ*408-480_GSG) retrotranslocation, related to Figure 4

(A) Sequence alignment (T-Coffee[S8]) of Hrd1 from the indicated species. Bold residues highlight the region exchanged to form chimeras used in (Figures 4A, 4B, and 4C). **(B)** Expression levels of Hrd1 variants were determined by immunoblotting. *hrd1Δ* cells expressing the indicated Hrd1-3xFlag constructs were normalized to wild-type Hrd1(WT) (1, black dashed line). Total protein was visualized by stain-free technology as a loading control. Results are displayed as the mean+/- SEM. Individual values are biological replicates. **(C)** In vitro autoubiquitination of Hrd1^{Cy5} (blue) in a reconstituted proteoliposome system with externally-oriented CPY*-TM^{800} (orange), internally-oriented CPY*-TM^{Cy3} (magenta). Wild-type Hrd1 (WT-positive control), a retrotranslocation-defective Hrd1 (Hrd1(KRK)-negative control), or Hrd1(*Δ*408-480_GSG) were reconstituted and incubated with recombinant ubiquitination machinery for the indicated times. Samples were analyzed by SDS-PAGE and in-gel fluorescence scanning to visualize Hrd1. Red pixels indicate saturation of signal during the imaging. Related to (Figures 4E-4J), second replicate. **(D)** Quantification of (C), showing unmodified Hrd1^{Cy5} (at ~70 kDa). **(E)** As in (C) showing external CPY*-TM^{800}. **(F)** Quantification of (E), showing unmodified external CPY*-TM^{800} (at ~70 kDa). **(G)** As in (C) showing internal CPY*-TM^{Cy3}. **(H)** Quantification (G), showing unmodified internally CPY*-TM^{Cy3} (at ~70 kDa).

For this figure, the number of quantified replicates and individual values are shown in Table S8 and S9.

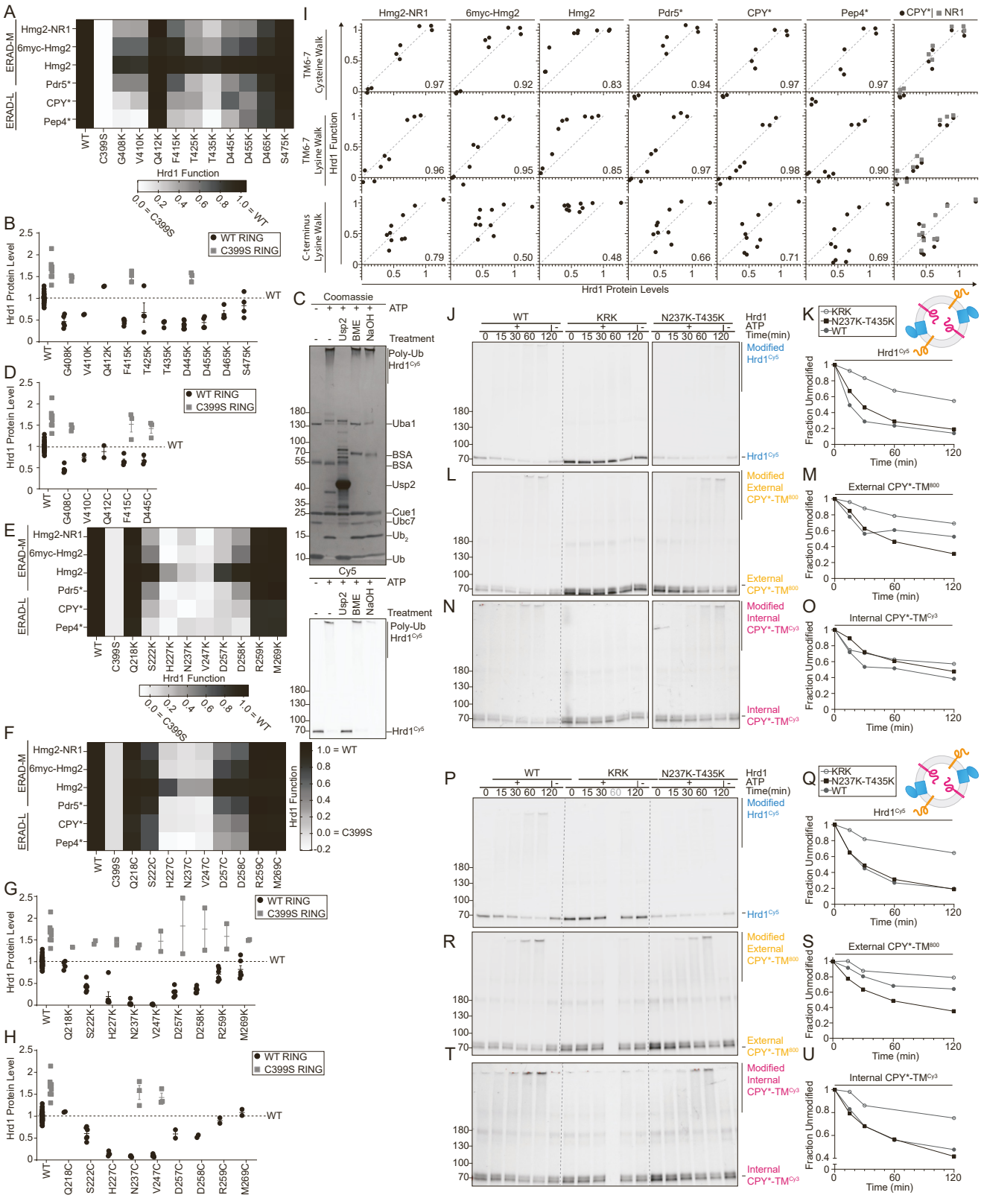

Figure S5. Stability-Function correlation of Hrd1 lysine substitutions, related to Figure 5
(Legend Next Page)

Figure S5. Stability-Function correlation of Hrd1 lysine substitutions, related to Figure 5
(A) Degradation of ERAD substrates by individual Hrd1 variants were followed by flow cytometry and summarized in a heatmap. The indicated Hrd1 variants were integrated in *hrd1Δ* cells expressing individual ERAD substrates and subjected to a 4-hour mid-log chase. Wild-type Hrd1(WT) is set to 1 (full function) and inactive Hrd1(C399S) is set to 0 (no function). Related to (Figure 5C). **(B)** Expression levels of Hrd1 variants were determined by immunoblotting. *hrd1Δ* cells expressing indicated Hrd1-3xFlag variants were normalized to wild-type Hrd1(WT) (1, black dash line). Total protein was visualized by stain-free technology as a loading control. Results are displayed as the mean +/- SEM. Individual values are biological replicates. Related to (Figures 5D and 5E). **(C)** Purified Hrd1(WT) in detergent micelles was incubated with recombinant ubiquitination machinery with or without ATP. After 60 minutes, the samples were treated with the indicated protein or chemical for 30 minutes at 37 °C. Samples were separated by non-reducing SDS-PAGE. Top: Coomassie staining of the in vitro ubiquitination reactions. Bottom: $Hrd1^{Cy5}$ fluorescence scanning. These data suggest that Hrd1 primarily autoubiquitinates on lysine residues but not cysteine residues (β-mercaptoethanol (BME) treatment) nor serine/ threonine residues (NaOH treatment) because these treatments did not reduce the ubiquitinated Hrd1 species. Note Hrd1 runs near 70 kDa, but is near the Coomassie limit of detection. Also, note that the NaOH treatment inactivated the Cy5 fluorophore. **(D)** As in (B). **(E)** As in (A) related to (Figure 5G). **(F)** As in (A). **(G)** As in (B), related to (Figure 5H-5J). **(H)** As in (B). **(I)** Correlation between Hrd1 protein levels and function for lysine and cysteine substitutions used in (Figures S5A, S5B, and S5E-S5H). Hrd1 protein levels were normalized to wild-type Hrd1 (set to 1) along the x-axis. The y-axis shows Hrd1 function as determined by flow cytometry normalized to inactive Hrd1(C399S) (0) and wild-type Hrd1 (1). Correlation coefficients (Pearson) are displayed in the bottom right corner of each. The gray dashed line demonstrates the trendline for a hypothetical 1:1 ratio of Hrd1 function:protein level. The right column of panels is an overlay of ERAD-L substrate CPY* (black circles) and ERAD-M substrate Hmg2-NR1 (gray squares). **(J)** In vitro autoubiquitination of $Hrd1^{Cy5}$ (blue) in a reconstituted proteoliposome system with externally-oriented CPY*-TM^{800} (orange), internally-oriented CPY*-TM^{Cy3} (magenta). Wild-type Hrd1 (WT-positive control), a retrotranslocation-defective Hrd1 (Hrd1(KRK)-negative control), or Hrd1(N237K-T435K) were reconstituted and incubated with recombinant ubiquitination machinery for the indicated times. Samples were analyzed by SDS-PAGE and in-gel fluorescence scanning to visualize Hrd1. Red pixels indicate saturation of signal during the imaging. Related to (Figures 5M-5R), second replicate. **(K)** Quantification of (J), showing unmodified $Hrd1^{Cy5}$ (at ~70 kDa). **(L)** As in (J) showing external CPY*-TM^{800}. **(M)** Quantification of (L), showing unmodified external CPY*-TM^{800} (at ~70 kDa). **(N)** As in (J) showing internal CPY*-TM^{Cy3}. **(O)** Quantification (N), showing unmodified internal CPY*-TM^{Cy3} (at ~70 kDa). **(P)** As in (J) showing $Hrd1^{Cy5}$, third replicate. Note: Hrd1(KRK) timepoint 60 (gray) was misloaded. **(Q)** Quantification of (P), showing unmodified $Hrd1^{Cy5}$ (at ~70 kDa). **(R)** As in (P) showing external CPY*-TM^{800}. **(S)** Quantification of (R), showing unmodified external CPY*-TM^{800} (at ~70 kDa). **(T)** As in (P) showing internal CPY*-TM^{Cy3}. **(U)** Quantification (T), showing unmodified internal CPY*-TM^{Cy3} (at ~70 kDa).

For this figure, the number of quantified replicates and individual values are shown in Table S8 and S9.

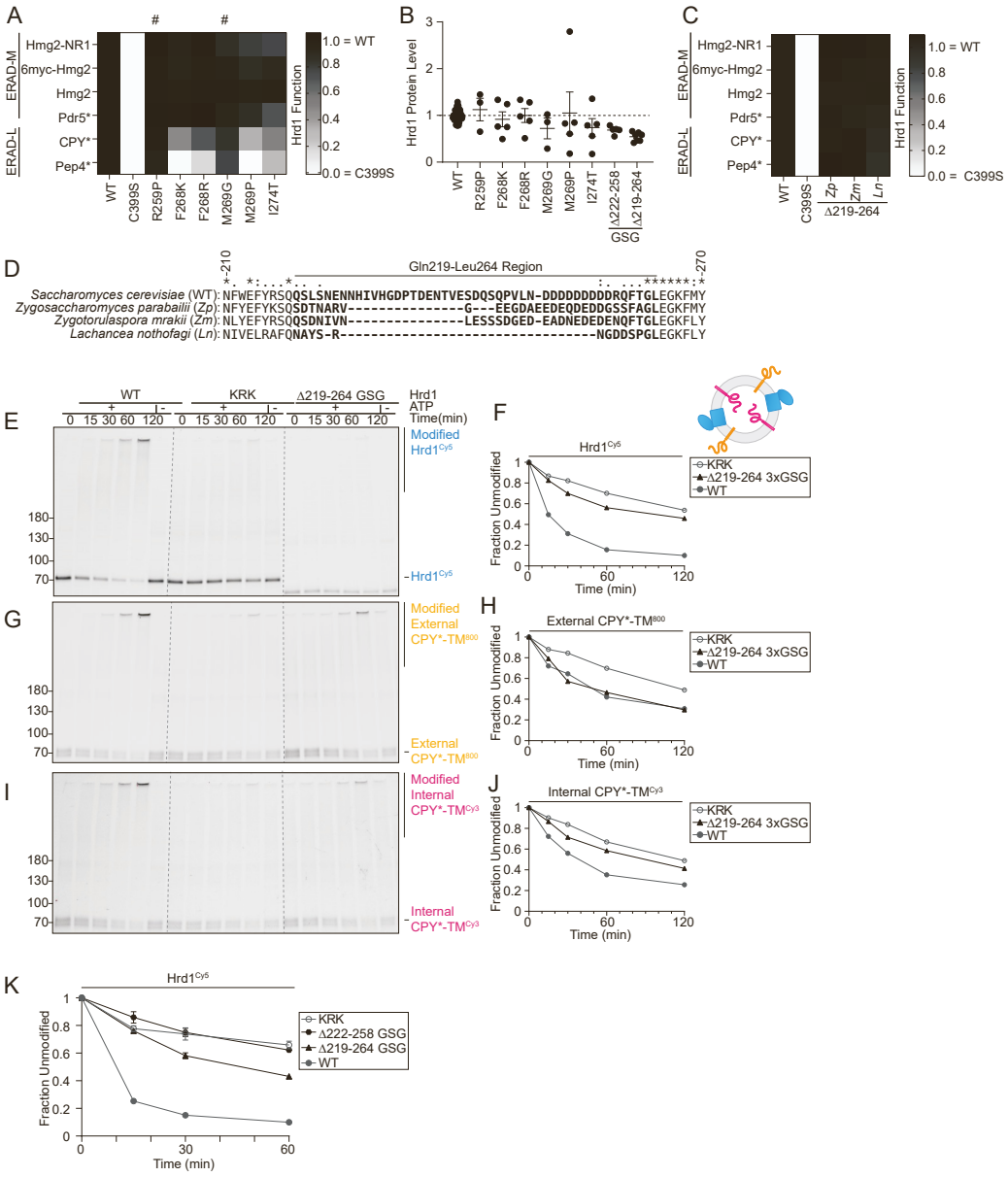

Figure S6. In vivo and in vitro analysis of the cytosolic loop between transmembrane segments 6 and 7, related to Figure 6

(A) Degradation of ERAD substrates by individual Hrd1 variants were followed by flow cytometry and summarized in a heatmap. The indicated Hrd1 variants were integrated in *hrd1Δ* cells expressing individual ERAD substrates and subjected to a 4-hour mid-log chase. Wild-type Hrd1(WT) is set to 1 (full function) and inactive Hrd1 is set to 0 (no function). "#" indicates a false positive hit. Related to (Figure 6A). **(B)** Expression levels of Hrd1 variants were determined by immunoblotting. *hrd1Δ* cells expressing indicated Hrd1-3xFlag variants were normalized to wild-type Hrd1(WT) (1, black dash line) . Total protein was visualized by stain-free technology as a loading control. Results are displayed as the mean +/- SEM. Individual values are biological replicates. **(C)** As in (A). Related to (Figure 6C). (Next Page)

Figure S6. In vivo and in vitro analysis of the cytosolic loop between transmembrane segments 6 and 7, related to Figure 6

(D) Sequence alignment (T-Coffee[S8]) of Hrd1 from the indicated species. Bold residues highlight the region exchanged to form chimeras used in (Figures 6C and S6C). **(E)** In vitro autoubiquitination of $Hrd1^{Cy5}$ (blue) in a reconstituted proteoliposome system with externally-oriented CPY*-TM^{800} (orange), internally-oriented CPY*-TM^{Cy3} (magenta). Wild-type Hrd1 (WT-positive control), a retrotranslocation-defective Hrd1 (Hrd1(KRK)-negative control), or Hrd1(Δ219-264_3xGSG) were reconstituted and incubated with recombinant ubiquitination machinery for the indicated times. Samples were analyzed by SDS-PAGE and in-gel fluorescence scanning to visualize Hrd1. Red pixels indicate saturation of signal during the imaging. Related to (Figures 6E-6J), second replicate. **(F)** Quantification of (E), showing unmodified $Hrd1^{Cy5}$ (at ~70 kDa). **(G)** As in (E) showing external CPY*-TM^{800}. **(H)** Quantification of (G), showing unmodified external CPY*-TM^{800} (at ~70 kDa). **(I)** As in (E) showing internal CPY*-TM^{Cy3}. **(J)** Quantification (I), showing unmodified internal CPY*-TM^{Cy3} (at ~70 kDa). **(K)** In vitro autoubiquitination of $Hrd1^{Cy5}$ or the indicated Hrd1 variants in detergent micelles. Hrd1 was incubated with recombinant ubiquitination machinery for the indicated times. Samples were analyzed by SDS-PAGE and in-gel fluorescence scanning to visualize Hrd1. The fraction of unmodified $Hrd1^{Cy5}$ was quantified and plotted. Data from three replicates displayed as mean +/- SEM.

For this figure, the number of quantified replicates and individual values are shown in Table S8 and S9.

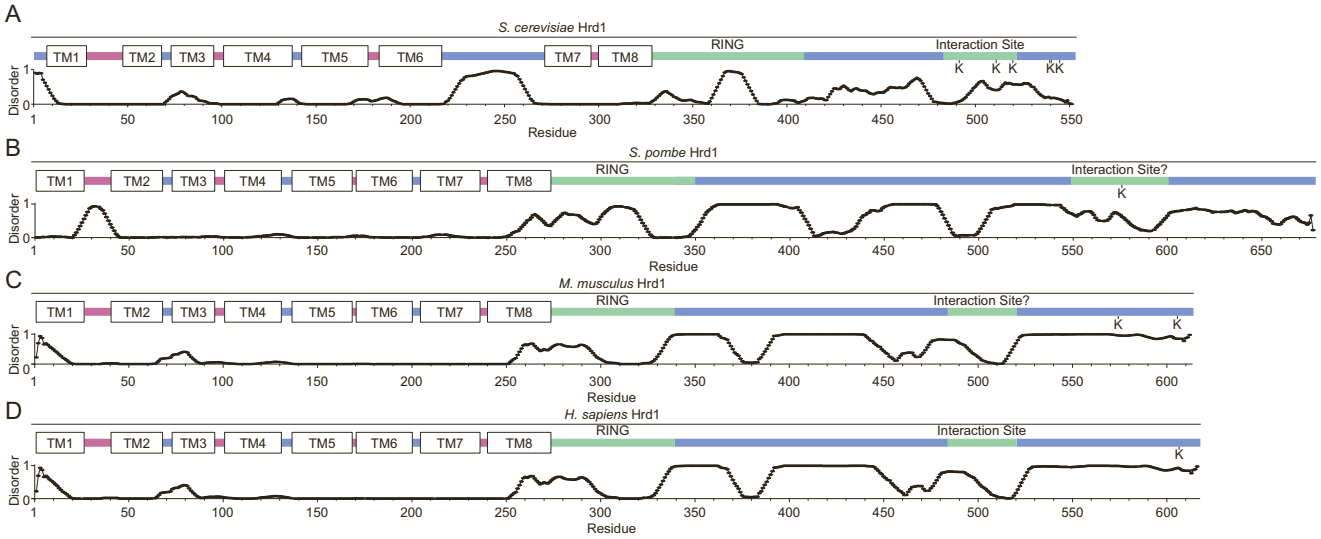

Figure S7. Hrd1 disorder predictions, related to Figure 7

(A) Top: Topology diagram of *S. cerevisiae* Hrd1 with transmembrane segments displayed as TM1-8. Colors indicate the cytosolic (blue), lumenal (magenta), cytosolic RING domain (green), and interaction site (green) is the Usa1 binding site. Bottom: Line chart representing predicted disorder (PONDR VLXT[S9]) of *S. cerevisiae* Hrd1 normalized 0 (ordered) to 1 (disordered). The location of lysine residues are indicated in the C-terminal region. Note that there are no cysteine residues in the C-terminal region. **(B)** As in (A) for *S. pombe.* Probable protein interaction site defined by predicted secondary structure in the C-term. **(C)** As in (A) for *M. musculus* Hrd1. Probable protein interaction site inferred from homology of *H. sapiens* Hrd1. **(D)** As in (A) for *H. sapiens* Hrd1. Protein interaction site is for HERP and FAM8A1.[S10]

Table S1. FACS Statistics, Related to Figure 1

Transformation number and sorting statistics for Hrd1 deep mutational scanning experiment. 'Cells Passing FACS Gates' are number of events (cells) passing FSC, SSC, and viability gates that were sorted over during FACS. 'WT Bin Cells Sorted' are number of events that were sorted into the wildtype-like bin. 'ERAD-L Defective Bin Cells Sorted' are number of events that were sorted into the ERAD-L defective bin. 'Second Sort Required ERAD-L Defective' indicates whether two rounds of FACS were required to get an ERAD-L defective population. If a second sort occurred, 'ERAD-L Defective Bin Cells Sorted' represents the number of cells in the first sort. 'No Replicate' is used to show missing populations.

Region	Amino Acids Mutated	Replicate	Transformation Number	Cells Passing FACS Gates	WT Bin Cells Sorted	ERAD-L Defective Bin Cells Sorted	Second Sort Required ERAD-L Defective
Region1	1-110	Rep1	114000	3397270	592201	4802	yes
Region1	1-110	Rep2	130600	5080021	754439	9810	yes
Region1	1-110	Rep3	830000	7723759	743912	2131	yes
Region1	1-110	Rep4	340000	6639568	745684	2064	yes
Region2	111-220	Rep1	75500	4568562	748316	No Replicate	
Region2	111-220	Rep2	28100	4739619	754568	913	yes
Region2	111-220	Rep3	1100000	6555795	744688	78	yes
Region2	111-220	Rep4	290000	7326345	746546	No Replicate	
Region3	221-330	Rep1	195100	4402482	752287	1352	yes
Region3	221-330	Rep2	37300	4319448	262462	No Replicate	
Region3	221-330	Rep3	1200000	6990509	734808	No Replicate	
Region3	221-330	Rep4	1039000	7140949	746182	123	yes
Region4	331-440	Rep1	25000	3418051	539993	10394	
Region4	331-440	Rep2	No Replicate	No Replicate	No Replicate	No Replicate	
Region4	331-440	Rep3	305000	6742996	596764	11163	
Region4	331-440	Rep4	542000	6889093	682226	11699	
Region5	441-551	Rep1	113000	4291029	750780	193524	
Region5	441-551	Rep2	66900	5002635	759250	210163	
Region5	441-551	Rep3	1020000	6467964	No Replicate	142180	
Region5	441-551	Rep4	680000	7269643	749054	138113	
		Min	25000	3397270	262462	78	
		Max	1200000	7723759	759250	210163	
		Median	290000	6467964	745933	9810	
		Mean	427973	5735038	689120	49234	

Table S13. Primers Library Generation, Related to STAR Methods

PCR setup for library creation. Each region of the library was created by two rounds of PCR. The first round forward and reverse primers are listed. In the second round of PCR, the products from round 1 PCR were combined with additional flanking forward and reverse primer.

		Round 1 PCR Fragment 1		Round 1 PCR Fragment 2				
Region	**Amino Acids Mutated**	**Flanking Forward Primer**	**Reverse Primer Pool**	**Forward Primer Pool**	**Flanking Reverse Primer**	**5' Homology (base pairs)**	**3' Homology (base pairs)**	**Vector (linearized with EcoRI)**
1	1-110	prBGP268	Pool A	Pool B	prBGP529	140	28	pBGP615
2	111-220	prBGP530	Pool C	Pool D	prBGP214	24	211	pBGP616
3	221-330	prBGP71	Pool E	Pool F	prBGP25	160	164	pBGP617
4	331-440	prBGP534	Pool G	Pool H	prBGP535	25	25	pBGP618
5	441-551	prBGP536	Pool I	Pool J	prBGP537	25	40	pBGP619

Supplemental References

S1. Bindels, D.S., Haarbosch, L., van Weeren, L., Postma, M., Wiese, K.E., Mastop, M., Aumonier, S., Gotthard, G., Royant, A., Hink, M.A., and Gadella, T.W., Jr. (2017). mScarlet: a bright monomeric red fluorescent protein for cellular imaging. Nat Methods 14, 53-56. 10.1038/nmeth.4074.

S2. Fisher, A.C., and DeLisa, M.P. (2008). Laboratory evolution of fast-folding green fluorescent protein using secretory pathway quality control. PLoS One 3, e2351. 10.1371/journal.pone.0002351.

S3. Plemper, R.K., Egner, R., Kuchler, K., and Wolf, D.H. (1998). Endoplasmic Reticulum Degradation of a Mutated ATP-binding Cassette Transporter Pdr5 Proceeds in a Concerted Action of Sec61 and the Proteasome. Journal of Biological Chemistry 273, 32848-32856. 10.1074/jbc.273.49.32848.

S4. Egner, R., Rosenthal, F.E., Kralli, A., Sanglard, D., and Kuchler, K. (1998). Genetic Separation of FK506 Susceptibility and Drug Transport in the Yeast Pdr5 ATP-binding Cassette Multidrug Resistance Transporter. Molecular Biology of the Cell 9, 523-543. 10.1091/mbc.9.2.523.

S5. Hampton, R.Y., and Rine, J. (1994). Regulated degradation of HMG-CoA reductase, an integral membrane protein of the endoplasmic reticulum, in yeast. J Cell Biol 125, 299-312. 10.1083/jcb.125.2.299.

S6. Shearer, A.G., and Hampton, R.Y. (2005). Lipid-mediated, reversible misfolding of a sterol-sensing domain protein. The EMBO Journal 24, 149-159. 10.1038/sj.emboj.7600498.

S7. Finger, A., Knop, M., and Wolf, D.H. (1993). Analysis of two mutated vacuolar proteins reveals a degradation pathway in the endoplasmic reticulum or a related compartment of yeast. European Journal of Biochemistry 218, 565-574. 10.1111/j.1432-1033.1993.tb18410.x.

S8. Notredame, C., Higgins, D.G., and Heringa, J. (2000). T-coffee: a novel method for fast and accurate multiple sequence alignment. Journal of Molecular Biology 302, 205-217. 10.1006/jmbi.2000.4042.

S9. Romero, P., Obradovic, Z., Li, X., Garner, E.C., Brown, C.J., and Dunker, A.K. (2001). Sequence complexity of disordered protein. Proteins: Structure, Function, and Bioinformatics 42, 38-48. 10.1002/1097-0134(20010101)42:1<38::AID-PROT50>3.0.CO;2-3.

S10. Schulz, J., Avci, D., Queisser, M.A., Gutschmidt, A., Dreher, L.-S., Fenech, E.J., Volkmar, N., Hayashi, Y., Hoppe, T., and Christianson, J.C. (2017). Conserved cytoplasmic domains promote Hrd1 ubiquitin ligase complex formation for ER-associated degradation (ERAD). Journal of Cell Science 130, 3322-3335. 10.1242/jcs.206847.

S11. Baldridge, R.D., and Rapoport, T.A. (2016). Autoubiquitination of the Hrd1 Ligase Triggers Protein Retrotranslocation in ERAD. Cell 166, 394-407. 10.1016/j.cell.2016.05.048.

S12. Stein, A., Ruggiano, A., Carvalho, P., and Rapoport, T.A. (2014). Key steps in ERAD of luminal ER proteins reconstituted with purified components. Cell 158, 1375-1388. 10.1016/j.cell.2014.07.050.

S13. Sikorski, R.S., and Hieter, P. (1989). A System of Shuttle Vectors and Yeast Host Strains Designed for Efficient Manipulation of DNA in Saccharomyces ceravisiae. Genetics 122, 19-27.
S14. Chen, I., Dorr, B.M., and Liu, D.R. (2011). A general strategy for the evolution of bond-forming enzymes using yeast display. Proc Natl Acad Sci U S A 108, 11399-11404. 10.1073/pnas.1101046108.
S15. Kapust, R.B., Tözsér, J., Fox, J.D., Anderson, D.E., Cherry, S., Copeland, T.D., and Waugh, D.S. (2001). Tobacco etch virus protease: mechanism of autolysis and rational design of stable mutants with wild-type catalytic proficiency. Protein Engineering, Design and Selection 14, 993-1000. 10.1093/protein/14.12.993.
S16. Hwang, J., Peterson, B.G., Knupp, J., and Baldridge, R.D. (2023). The ERAD system is restricted by elevated ceramides. Science Advances *9*, eadd8579. 10.1126/sciadv.add8579.